Origins of gas discharging from the Qiangtang Basin in the northern Qinghai–Tibet Plateau, China: Evidence from gas compositions, helium, and carbon isotopes

Min Luo [a,d], Huagu Huang [a,c,d], Peng Zhang [b], Qingbai Wu [b], Duofu Chen [a,*]

[a] Key Laboratory of Marginal Sea Geology, Guangzhou Institute of Geochemistry, Chinese Academy of Sciences, Guangzhou 510640, China
[b] Cold and Arid Regions Environmental and Engineering Research Institute, Chinese Academy of Sciences, Lanzhou 730000, China
[c] Guangdong Geologic Survey Institute, Guangzhou 510080, China
[d] University of Chinese Academy of Sciences, Beijing 100049, China

ABSTRACT

Gas compositions, helium isotopic ratios, and carbon isotopic compositions of CO_2 and CH_4 from six gas emission sites in the Qiangtang Basin and its adjacent areas were measured in order to unravel their origins. Gas samples from the Beiluhe, the Bucha Lake, and the eastern Tuotuo River are N_2-rich with N_2 over 75 vol.%, while the contents of CO_2 and CH_4 are only 3.45–20.91 vol.% and 0–3.58 vol.%, respectively. Relatively high $CO_2/^3He$ (~9.95×10^{11}) and $CH_4/^3He$ (5.9×10^9–1.65×10^{10}), and low $\delta^{13}C$ values of CO_2 (~-15.4‰) and CH_4 (~-29.7‰) suggest that both CO_2 and CH_4 from the Bucha Lake are biotic. The S–M–L (S, M, and L represent sedimentary organic carbon, mantle, and limestone, respectively.) three-component mixing model suggests that no mantle-derived CO_2 exists in these samples, which is consistent with the result that He in these gas samples is all crust-derived. CO_2 in gas samples from the Beiluhe and the eastern Tuotuo River are relatively enriched in ^{13}C of CO_2 ($\delta^{13}C$: -8.4‰ and -5.5‰) and low $CO_2/^3He$ (2.3×10^9 and 2.4×10^9) as well as $CH_4/^3He$ (5.9×10^7 and 3.4×10^7) ratios. These patterns suggest that both CO_2 and CH_4 are abiotic, demonstrated by the S–M–L three-component mixing model displaying that more than 50% CO_2 in these two sites are mantle-derived. CO_2-rich gases are discovered in the southern Erdaogou Depot, the branch of Tuotuo River, and the Tanggula Mountain Depot with CO_2 exceeding 96 vol.%. The relatively high $\delta^{13}C$ of CO_2 (-4.2 to -7.7‰), low $CO_2/^3He$ ratios (7.9×10^8–9.3×10^9), as well as the S–M–L three-component mixing model reveal that CO_2 at least partially originates from the mantle source. Only one gas sample from the Tanggula Mountain Depot contains a trace amount of abiotic CH_4 ($CH_4/^3He = 1.2 \times 10^7$) generated by abiotic reduction of mantle-derived CO_2. However, the source of He is dominantly crust-derived with only 2.15–5.66% mantle-derived He. The emission of large quantity of mantle-derived CO_2 is likely due to the presence of the Hoh Xil–Jinsha River suture and the Cenozoic volcanism in northern Tibet. Nevertheless, the small fraction of mantle-derived He may result from the limited degree of openness at the bottom of fault zones and possibly reflect a geological setting of strong extrusion and crustal thickening.

1. Introduction

Gas discharge is ubiquitous worldwide and its related geological phenomena are also widespread in both terrestrial and marine environments, such as mud volcanoes, hot springs, pockmarks, and cold seeps (Etiope et al., 2009; Judd and Hovland, 2007). Geochemical studies of discharging gases, including measuring gas species, concentrations, and isotopic compositions, play a significant role in the exploration of hydrocarbon and gas hydrate, in monitoring tectonic and magmatic activities, and in the environmental effect assessment of greenhouse gases (Bräuer et al., 2009; Etiope and Klusman, 2002; Yang, 2008, 2013; Yang et al., 2010). The analysis of carbon isotopes is one of the most direct and effective ways to fingerprint the origin of emitting gases. Moreover, concentrations and isotopic ratios of noble gases that provide information about the source of fluids are widely applied in the study of crust–mantle interaction, geotectonics, terrestrial heat flow, etc. (Battani et al., 2000; Holland and Ballentine, 2006; Lollar and Ballentine, 2009; Xu et al., 1996, 2003; Yang et al., 2009).

Previous studies associated with surface gas manifestations in the Qinghai–Tibet Plateau are mainly focused on the geothermal gases in the southern and central Tibetan Plateau. Helium in hot spring gases from Yangbajain and its adjacent areas in southern Tibet consist of both crust-derived and mantle-derived helium and $\delta^{13}C_{CO_2}$ values also show that the CO_2 are multi-sourced (Yokoyama et al., 1999). Zhao et al. (2002) found that most of the hydrothermal activities occurred in the

southern side of the Banggonghu–Nujiang suture and two types of geothermal gases can be distinguished, i.e. CO_2-enriched and N_2-enriched gases. They also detected helium of mantle origin at the Moincer hot spring, which indicates a mantle component at shallow crustal depth. Hoke et al. (2000) defined two principal domains in the southern Tibetan Plateau based on the isotopic composition of helium. Their suggested boundary, about 50–100 km north of the Brahmaputra suture zone, is not only regarded as the southern limit of recent mantle melting and mantle melt extraction beneath the Tibetan Plateau, but also inferred to coincide with the junction between the Indian and Asian Plates. However, Hou and Li (2004) asserted that the of principal domains based on helium isotope variations are divided along the 89°E longitude in the east–west direction rather than in the south–north direction. To the west of 89°E divide, the continental slab, gently dipping in NNE direction, has probably passed the Brahmaputra suture, whereas to the east of 89°E, an underthrusting slab front is subducted in a steep slope, and thus has not spanned the Brahmaputra suture. In addition, CH_4 discharging from cold emissions was discovered in the Tuojiu Mountain, the Kunlun Pass, and Yanshiping, which was attributed to possible gas hydrate occurrence in these regions (Lu et al., 2007).

The Qiangtang Basin is located in the northern Qinghai–Tibet Plateau with an average altitude of more than 5000 m. So far, the surface gas manifestations have been poorly investigated due to difficulties accessing northern Tibet and its severe natural condition. In the present study, we report for the first time field investigations on eight gas emission sites in the Qiangtang Basin and its adjacent areas. We present gas compositions, stable carbon isotopic ratios of CO_2 and CH_4, as well as helium isotopic composition from six gas emission sites in order to trace the origin of the discharging gases. We also provide some basic

geochemical data of surface gas manifestations for studying the tectonic evolution of the Qiangtang Basin and supporting hydrocarbon and gas hydrate exploration in the Qiangtang Basin.

2. Geological setting

The Qiangtang Basin covers a region of approximately 18.5×10^4 km^2 (~300 km wide and ~640 km long) in the north-central Qinghai–Tibet Plateau (Wang and Yi, 2001). Sandwiched between the Gangdise-Nyainqentanglha plate and the Hoh Xil-Bayan Har plate, and bounded by the Hoh Xil–Jinsha River suture zone to the north and the Bangong Lake–Nujiang River suture zone to the south, the Qiangtang Basin consists of the Northern Qiangtang depression, the Central Uplift, and the Southern Qiangtang depression (Huang, 2001) (Fig. 1). It developed on the pre-Paleozoic crystalline basement and Paleozoic fold basement and evolved to a foreland basin during the Triassic and Jurassic. Since the Cretaceous, the Bangong Ocean closed by northward subduction beneath the Qiangtang terrane and a large-scale regression occurred in the Qiangtang Basin, leading to the uplift and denudation of the basin (Cai et al., 1996; Kapp et al., 2003). The late Permian, Triassic, and Jurassic oil-generating strata are the primary oil source rocks in the Qiangtang Basin which are currently in mature to overmature stage. They mainly distribute along the rim of the Central Uplift and in the central Northern and Southern Qiangtang depression and show a great potential for gas and oil formation. Moreover, hundreds of oil seepage sites have been discovered mainly in the central Qiangtang Basin (Nan et al., 2008). Thus, the Qiangtang Basin is considered as a favorable area for hydrocarbon exploration in northern Tibet (Wang et al., 2004; Zhao et al., 2001). In addition, in consideration of the gas sources, transportation and reservoir
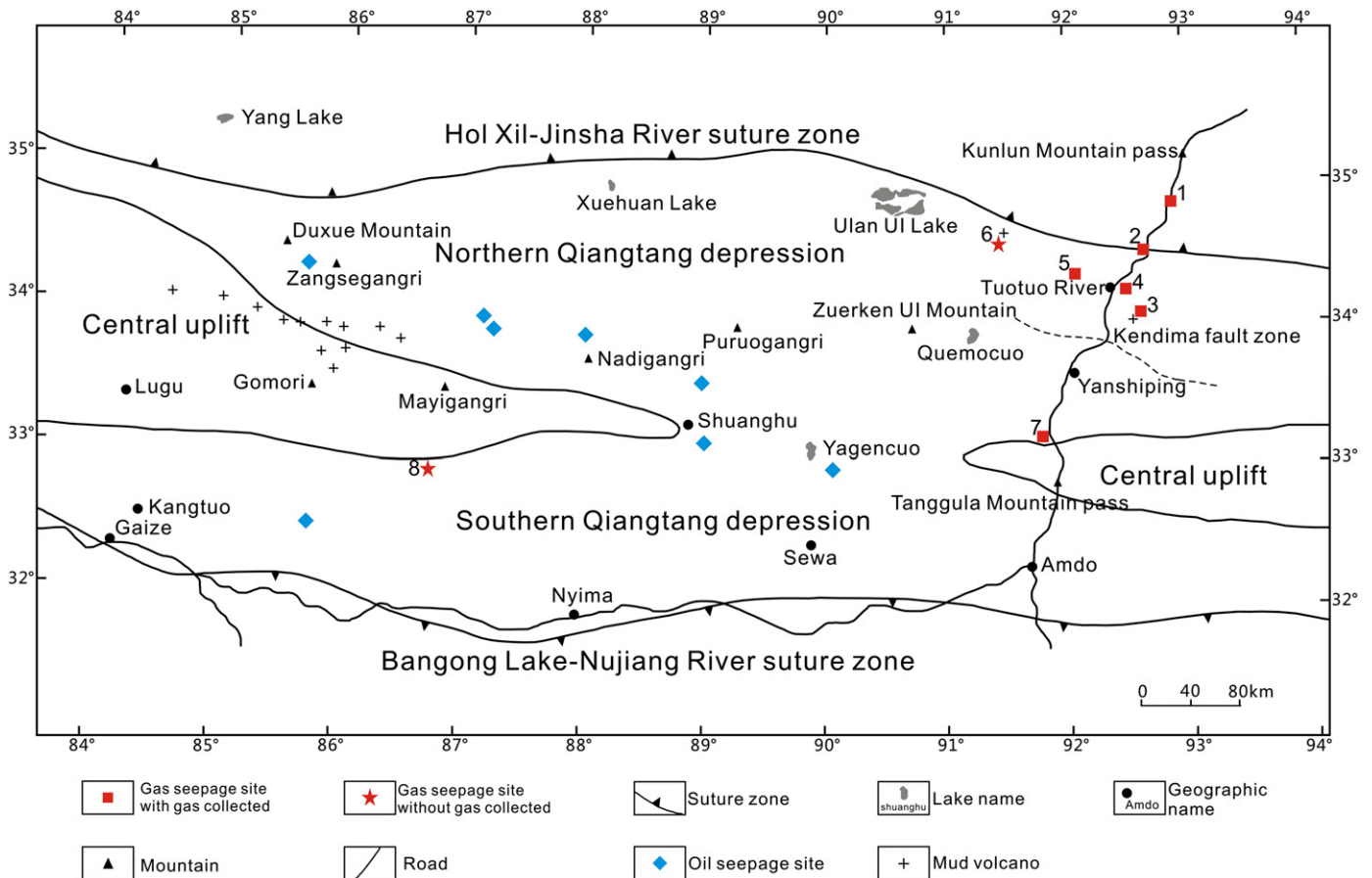

Fig. 1. Tectonic units of the Qiangtang Basin and the distribution of the investigated gas emission sites (modified from Xia (2009)). The distribution of mud volcanoes is according to Hu and Zhang (1998) and Xie et al. (2009), and the occurrences of oil seepage sites are taken from Nan et al. (2008). Note that only major focused oil seepage sites are shown. Names of gas emission sites: 1, the Beiluhe; 2, the southern Erdaogou Depot; 3, the Bucha Lake; 4, the eastern Tuotuo River; 5, the branch of Tuotuo River; 6, the northwestern Mazhangcuoqin; 7, the Tanggula Mountain Depot; and 8, the southwestern Rongmaxiang.
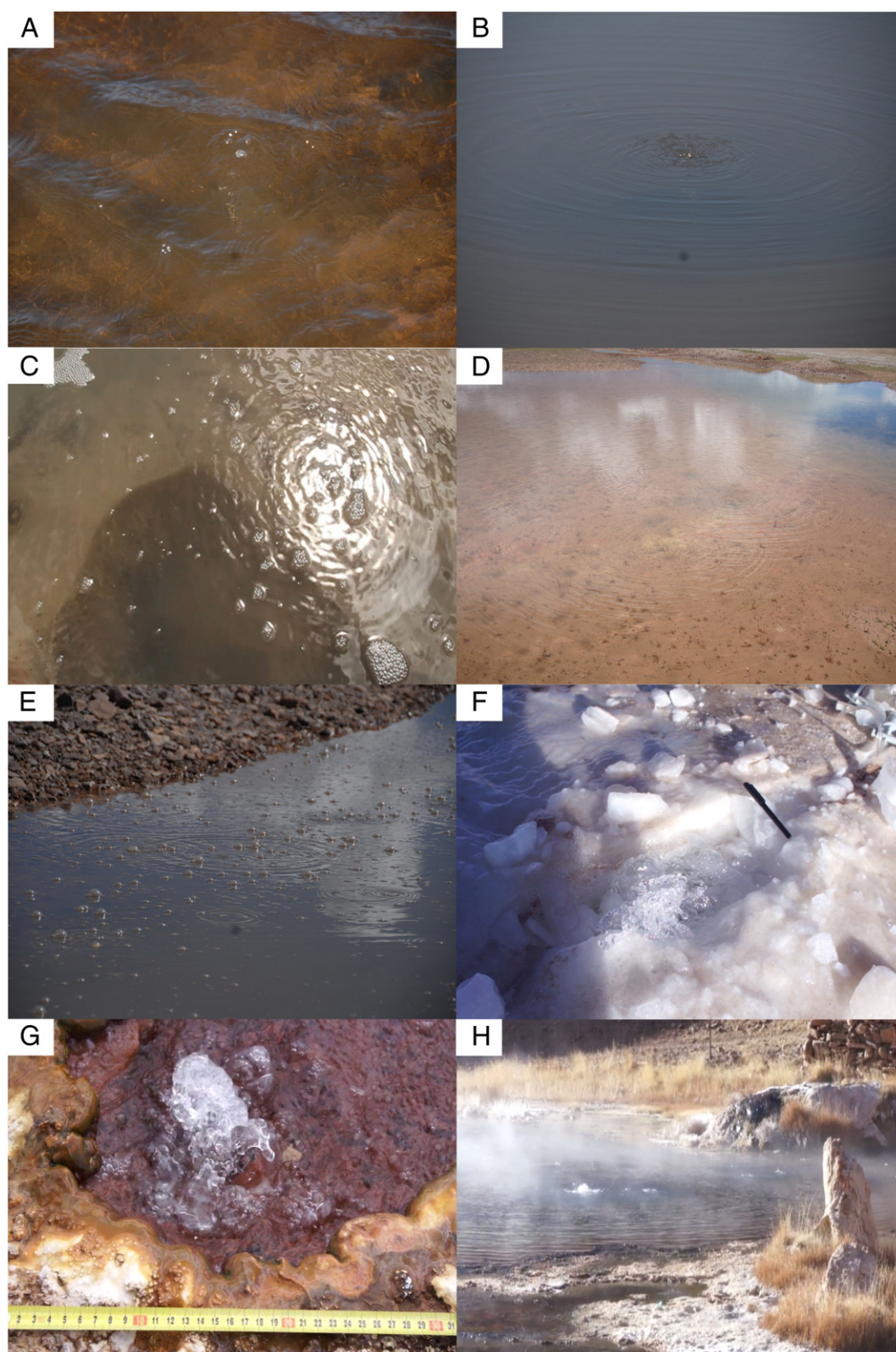
Fig. 2. Photographs of the eight investigated gas emission sites. (A) The Beiluhe. The bubbles ascend continuously from the water and the diameters of most bubbles are ~1 cm; (B) The southern Erdaogou Depot. Most bubbles rise continuously from the water and their diameters are no more than 2 cm; (C) The Bucha Lake. The gas bubbles intensely and continuously emit from the water with their diameters of 1–5 cm; (D) The eastern Tuotuo River. The gas discharges continuously from the water with the bubbles' diameters of 1–3 cm; (E) The branch of Tuotuo River. A stretch of continuous gas emission with the bubbles' diameters of 1–3 cm is observed; (F) The northwestern Mazhangcuoqin. The gas emission site is situated on a mud volcano with its crater's diameter of 25–30 m. The gas and water expulse drastically after the ice is broken; (G) The Depot of Tanggula Mountain. The water temperature is about 38–40 °C and the bubbles emit continuously and intensely from the water with their diameters of 1–5 cm. Yellow–gray travertine is observed around the vents; (H) The southwestern Rongmaxiang. The gas and water of ~40 °C emit continuously and intensely with the bubbles' diameters of 1–5 cm. The pictures of gas emission sites A, B, C, D, E, and G were taken in August, 2011, and the pictures of gas emission sites F and H were taken in December, 2011.

Table 1
Gas compositions and their carbon isotopic ratios.

Sample numbers	Sampling sites	N_2 (%)	CO_2 (%)	CH_4 (%)	C_2H_6 (%)	C_3H_8 (%)	$\delta^{13}C_1$[a] (PDB, ‰)	$\delta^{13}C_2$[a] (PDB, ‰)	$\delta^{13}C_{CO_2}$ (PDB, ‰)
G1	Beiluhe	82.59	13.80	3.58	0.02	0.01	−28.3	–	−8.4
G2	Southern Erdaogou Depot	0.00	99.41	0.59	0.00	0.00	–	–	−6.7
G3		0.00	99.97	0.03	0.00	0.00	–	–	−4.8
G4		0.00	>99.99	0.00	0.00	0.00	–	–	−7.6
G5		0.00	99.99	0.01	0.00	0.00	–	–	−5.2
G6	Bucha Lake	96.07	3.64	0.22	0.06	0.01	−29.7	−20.5	−15.1
G7		95.50	3.84	0.64	0.1	0.01	−29.7	−18.0	−15.9
G8		96.55	3.45	0.01	0.00	0.00	−29.6	–	−15.2
G9	Eastern Tuotuo River	78.79	20.91	0.30	0.00	0.00	–	–	−5.5
G10	Branch of Tuotuo River	0.00	>99.99	0.00	0.00	0.00	–	–	−7.7
G11	Tanggula Mountain Depot	3.12	96.77	0.11	0.00	0.00	−27.7	–	−4.5
G12		1.46	98.54	0.01	0.00	0.00	–	–	−4.2

[a] $\delta^{13}C_1$ and $\delta^{13}C_2$ represent the $\delta^{13}C$ values of methane and ethane, respectively.

conditions, the Qiangtang Basin should be the best prospective region for gas hydrate occurrence (He et al., 2012; Zhu et al., 2011).

3. Sampling and methods

Twelve gas samples were collected from the six gas emission sites in the Qiangtang Basin and its adjacent areas (Figs. 1&2). Cylindroid glass bottles with a frosted piston switch at each end of the bottle were used to collect the seeping gas. A funnel with a rubber tube connected to a hand-operated vacuum pump was inverted upon the bubbles in the water. Air was continuously pumped out of the glass bottle, and then the seeping gas was introduced slowly into the bottle by using the hand-operated vacuum pump through the rubber tube. After an adequate amount of gas was collected, the frosted piston switch was turned off and the gas samples were transported to the Key Laboratory of Gas Geochemistry (Lanzhou), Institute of Geology and Geophysics, Chinese Academy of Sciences as soon as possible for geochemical analysis.

Gas compositions were analyzed by HP5890II gas chromatography system equipped with a flame ionic detector and thermal conductivity. The analytical precision for major gas constituents is ±5%. Carbon isotopic compositions of CO_2 and CH_4 were determined using a continuous flow isotope ratio mass spectrometer (Finnigan Delta plus XP). The carbon isotopic ratios are expressed by the conventional delta notation in per mil (‰) with respect to PDB (Pee Dee Belemnite from South Carolina). The measurement errors for carbon isotopic ratios are ±0.2‰. Helium isotopic compositions were measured by a MM5400 mass spectrometer. The accuracy of helium isotopic results was checked by repeatedly measuring the standard air collected from the top of Gaolan Mountain in Lanzhou City, China. Hot-blanks with $^4He = 2.46 \times 10^{-10}$ and $^{20}Ne = 4.08 \times 10^{-10}$ at 1600 °C (cm³ STP) were run using the same procedure as the real samples, and all the results were calibrated to hot-blank. Details of analytical procedures and errors were described in reference Ye et al. (2007).

4. Results

4.1. Characteristics of gas emission sites and gas compositions

The gas emission site of the Beiluhe is located near the Qinghai–Tibet Highway in front of the Beiluhe Base of Cold and Arid Regions Environmental and Engineering Research Institute, Chinese Academy of Sciences. The bubbles ascend continuously from the water and most of them are ~1 cm in diameter (E92°56′19.8″, N34°49′44.8″, 4633 m in altitude) (Fig. 2A). Gas sample from the Beiluhe (G1) is N_2-dominant with the proportion of 82.59 vol.%. It also contains small amounts of CO_2 (13.80 vol.%) and CH_4 (3.58 vol.%), and trace amounts of C_2H_6 (0.02 vol.%) as well as C_3H_8 (0.01 vol.%) (Table 1).

The gas emission site of the southern Erdaogou Depot was found in the flood plain of Herinachiqu River. Gas seeps continuously from the

water. The diameter of the bubbles is typically smaller than 2 cm (E92°44′51.5″, N34°35′37.7″, 4620 m in altitude) (Fig. 2B). Gas samples from the southern Erdaogou Depot (G2, G3, G4, and G5) have high content of CO_2 (99.41–99.99 vol.%) but low content of CH_4 (0.01–0.59 vol.%) (Table 1).

The gas emission site of the Bucha Lake is located 48 km southwest of the Tuotuo River. Gas emits continuously and intensely from the water. Bubble diameters are between 1 and 5 cm (E92°40′54.1″, N34°03′05.4″, 4483 m in altitude) (Fig. 2C). Mud seepage was also seen expulsing from some fluid discharge outlets. N_2 (95.50–96.20 vol.%) is the major component of gas samples from the Bucha Lake (G6, G7, G8) and the contents of CO_2 are only 3.45–3.84 vol.% (Table 1).

The gas emission site of the eastern Tuotuo River was discovered 6 km away from the Tuotuo River, with gas seeping continuously from the water with the bubble-diameters of 1–3 cm (E92°33′45.0″, N34°12′10.1″, 4518 m in altitude) (Fig. 2D). The gas sample from the eastern Tuotuo River (G9) consists of N_2 (78.79 vol.%), CO_2 (20.91 vol.%), and CH_4 (0.3 vol.%) (Table 1).

The gas emission site of the branch of Tuotuo River is situated near the junction of the branches of Tuotuo River–Dongduoqu and Zhamuqu, 40 km northwestern away from the Tuotuo River. A stretch of continuous gas emission was observed with the bubble diameters of 1–3 cm (E92°07′30.8″, N34°18′46.6″, 4585 m in altitude) (Fig. 2E). The gas sample from the branch of Tuotuo River (G10) is almost comprised of pure CO_2 (Table 1).

The gas emission site of the Tanggula Mountain Depot is located on the hillside in proximity to the Tanggula Mountain Depot. The water temperature is about 38–40 °C. The gas and water discharge continuously and intensely with the bubbles' diameters of 1–5 cm (E91°51′04.3″, N33°08′30.6″, 4901 m in altitude) (Fig. 2G). Yellow–gray travertine was observed around the fluid outlets. The gas samples (G11, G12) are dominated by CO_2 with N_2 and CH_4 proportion of 1.46–3.12 vol.% and 0.01–0.11 vol.%, respectively (Table 1).

4.2. Isotopic compositions of discharging gases

$^3He/^4He$ values of the 11 gas samples range from 0.07×10^{-6} to 1.19×10^{-6}, and R/Ra values are between 0.05 and 0.85 (Ra is the $^3He/^4He$ ratio of air) (Table 2). It is necessary to adjust the $^3He/^4He$ values due to the possible air contamination during sampling. Assuming that all the ^{20}Ne concentration of the samples come from the atmosphere, we can correct the helium ratios for atmospheric helium contamination by Eq. (1) (Poreda and Craig, 1989).

$$\begin{aligned} \left(^3He/^4He\right)_c &= \left[\left(^3He/^4He\right)_s - \left(^3He/^4He\right)_{air} \times r\right]/(1-r) \\ r &= \left(^4He/^{20}Ne\right)_{air}/\left(^4He/^{20}Ne\right)_s \end{aligned} \quad (1)$$

where the subscript c is the corrected value; air is the value of air; and s is the measured value. Since $^4He/^{20}Ne$ ratio of G12 is quite close to the ratio

Table 2
Helium isotopic ratios of seeping gas.

Sample numbers	Sampling sites	$^4He/^{20}Ne$	$^3He/^4He$ ($\times 10^{-6}$)	R/Ra	Rc/Ra	Mantle-derived He (%)	$CO_2/^3He$ ($\times 10^{10}$)	$CH_4/^3He$ ($\times 10^8$)
G1	Beiluhe	7.47	0.43	0.31	0.28	2.86	0.23	0.59
G3	Southern Erdaogou Depot	2.50	0.54	0.39	0.30	3.14	0.36	–
G4		1.60	0.84	0.60	0.50	5.66	0.82	–
G5		1.72	0.65	0.47	0.35	3.77	0.93	–
G6	Bucha Lake	34.55	0.07	0.05	0.04	0	98.27	59.41
G7		34.39	0.07	0.05	0.04	0	99.84	165.25
G8		32.62	0.07	0.05	0.04	0	100.47	87.33
G9	Eastern Tuotuo River	0.52	1.00	0.72	0.27	2.77	0.24	0.34
G10	Branch of Tuotuo River	1.52	0.61	0.44	0.29	2.97	0.54	–
G11	Tanggula Mountain Depot	1.14	0.61	0.44	0.22	2.15	0.079	0.12
G12		0.39	1.19	0.85	0.18	1.67	0.13	–

of air (0.319) because of serious air contamination, it is not considered in the following discussion. The variation range of $^3He/^4He$ values diminishes after correction and Rc/Ra ratios are between 0.04 and 0.50 (Table 2).

$\delta^{13}C_{CO_2}$ values of the 11 gas samples from the six gas emission sites range from -15.9 to -4.5‰. $\delta^{13}C$ values of CH_4 in gas samples from the Beiluhe (G1), the Bucha Lake (G6, G7, G8), and the Tanggula Mountain Depot (G11) are between -29.7 and -27.7‰, and $\delta^{13}C$ values of C_2H_6 in gas samples from the Bucha Lake (G6, G7) are -20.5‰ and -18.0‰ (Table 1).

5. Discussion

5.1. Origin of helium

Helium has been commonly used as a fluid source tracer because it is chemically inert, physically stable, and highly mobile. It can travel in rock matrix, accumulate in the rock pores and fissures, and finally enter groundwater and atmosphere (Ozima and Podosek, 2002). The helium isotopic ratios of natural gases are typically defined by varying fractions of the three major components (1) air (homogeneous $^3He/^4He$ ratio of Ra = $\sim 1.40 \times 10^{-6}$), (2) crust ($^3He/^4He$ ratios of ~0.05Ra are much lower than that of air because abundant ^4He gases are produced by alpha decay of radioactive isotopes (^{238}U, ^{235}U, ^{232}Th)), and (3) mantle (characterized by high $^3He/^4He$ ratios of ~8Ra related to high amounts of primordial ^3He (Oxburgh et al., 1986; Porcelli

Fig. 3. $^3He/^4He$ vs. $^4He/^{20}Ne$ plot for the gas samples in this study and other places in China. Solid triangles denote gas samples in this study. Open squares and solid circles are the data of geothermal gas samples in Tengchong, SW China (Xu et al., 2004). Solid diamonds represent gas samples offshore NW Taiwan (Yang et al., 2005). Open circles denote hot spring gases in Hainan Island (Xu et al., 2012). Open diamonds denote geothermal gases in southern Tibet (Hoke et al., 2000). The mixing lines were calculated by using the formula according to Craig et al. (1978).

et al., 2002)). The relationship of $^3He/^4He$ and $^4He/^{20}Ne$ shows that gas samples from the Qiangtang Basin and its adjacent area mainly cluster along the mixing line of air–crust end-members (Fig. 3), reflecting a major contribution of radiogenic crustal He. Additionally, the relative proportion of mantle-derived He can be calculated according to Eq. (2) (Andrews, 1985):

$$He(\%) = \left[\left(^3He/^4He\right)_s - \left(^3He/^4He\right)_c / \left(^3He/^4He\right)_m - \left(^3He/^4He\right)_c \right] \quad (2)$$

where He (%) is the relative proportion of mantle-derived He; subscript s is the measured value; c is R/Ra value of crust-derived He (~0.05) (Morrison and Pine, 1955); and m is R/Ra value of mantle-derived He (~8) (Graham, 2002). The calculations also reveal that the radiogenic crustal helium is dominant in all gas samples in the investigated area, which are consistent with the results of the $^3He/^4He$–$^4He/^{20}Ne$ plot. He in measured samples from the Bacha Lake is crustal-radiogenic without the mixture of mantle-derived He. In contrast, gas samples from the Beiluhe, the eastern Tuotuo River, the branch of Tuotuo River, and the Tanggula Mountain Depot contain certain amounts of mantle-derived He (2.15–2.97%) (Table 2). Gas samples from the southern Erdaogou Depot exhibit the highest proportion of mantle-derived He (up to 5.66%), most likely because this gas emission site is in close proximity to deep seated fault zone — the Hoh Xil–Jinsha River suture zone (Fig. 1). This fault zone acts as a conduit for mantle-derived fluid to migrate to shallow crust, resulting in the relatively high mantle-derived He content in seeping gases. However, the proportion of mantle-derived He in the gas samples from the target area is much lower than those from the southern Tibet and the southwestern Yunnan, which possibly results from the limited degree of openness at the bottom of fault zones (Shen et al., 2007; Zhao et al., 2002) and reflects a geological setting of strong extrusion and crustal thickening (Li et al., 2011; Zhao et al., 2004). Alternatively, the small contribution from mantle-derived He may be caused by the dilution of radiogenic crustal He from U and Th decay in the continental crust.

5.2. Sources of CO_2

CO_2 in natural gases may be derived from various sources, including methanogenesis, oil field biodegradation, kerogen decarboxylation, hydrocarbon oxidation, decarbonation of carbonates, and magma degassing (Wycherley et al., 1999). The $\delta^{13}C_{CO_2}$ value can be used to distinguish between some of these sources. Biotic CO_2 generally has $\delta^{13}C_{CO_2}$ values below -10‰, whereas the abiotic CO_2 contains high amounts of heavy carbon, resulting in $\delta^{13}C_{CO_2}$ values above -8‰ (Song and Xu, 2005). Among them, the $\delta^{13}C$ of mantle-derived CO_2 associated with MORB falls within -6.5 ± 2‰ (Sano and Marty, 1995).

The average $\delta^{13}C_{CO_2}$ value of gas samples from the Bucha Lake is -15.4‰ (Table 1), indicating that CO_2 is biogenic in origin. The CO_2 in gas samples from the Beiluhe, the southern Erdaogou Depot, the eastern Tuotuo River, the branch of Tuotuo River, and the Tanggula Mountain
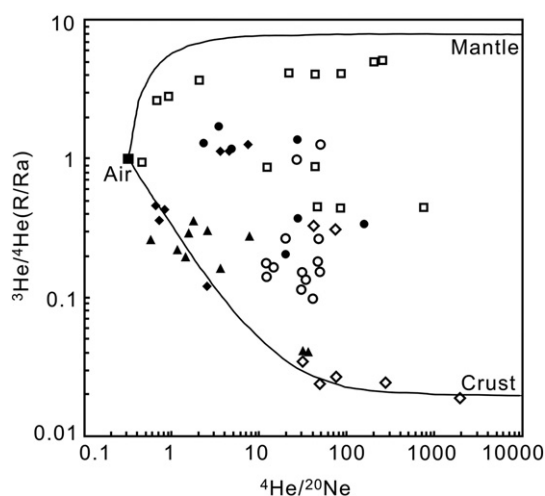
Depot is abiotic and could possibly be associated with mantle-derived fluid because their $\delta^{13}C_{CO_2}$ values (-4.5 to $-8.4‰$) fall within the range of MORB (Table 1). Dai et al. (1995) concluded that CO_2 in gas samples is abiotic in origin, if CO_2 concentrations are higher than 60 vol.% (based on synthesizing the concentrations and carbon isotopic compositions of CO_2 in 212 gas samples of different sources from China and in more than 100 gas samples from Australia, Thailand, New Zealand, Philippines, and Canada). The CO_2 contents of discharging gas from the southern Erdaogou Depot, the branch of Tuotuo River, and the Tanggula Mountain Depot are all greater than 90 vol.%, which further supports the hypothesis of the CO_2 being of abiotic origin.

Undoubtedly, the use of $\delta^{13}C_{CO_2}$ values has its limits in deciphering CO_2 origins due to the overlap over $\delta^{13}C_{CO_2}$ values from different sources. Hence, we combine other parameters to trace CO_2 origins. The $CO_2/^3He$ ratio can act as a sensitive indicator for fingerprinting carbon provenance since diagnostic values exist in the earth's various reservoirs (crust/mantle/atmosphere) (Crossey et al., 2009; Sherwood Lollar et al., 1997). The $CO_2/^3He$ ratios of collected gas samples vary over 3 orders of magnitude, from the range of 1×10^9 to 1×10^{10} (MORB-like) to higher values normally associated with crustal lithologies (Marty and Jambon, 1987; O'Nions and Oxburgh, 1988). According to Fig. 4 showing the $CO_2/^3He$ ratios plotted against CO_2 volume, a significant proportion of the CO_2 in all gas samples except those from the Bucha Lake is magmatic in origin. However, we cannot rule out the addition of some crustal-derived CO_2 to the reservoirs, particularly the two samples from the southern Erdaogou which almost cluster along the dividing line between mantle and crustal CO_2. The $CO_2/^3He$ ratios of gas samples from Tanggula Mountain Depot are below that of mantle-derived fluids, which is possibly caused by CO_2 loss due calcite precipitation since they were collected from hot springs with travertine around. In contrast, a large amount of N_2 in gas samples from the Beiluhe and the eastern Tuotuo River would lead to CO_2 dilution as shown in Fig. 4.

Assuming the CO_2 signatures in the study area result from the mixture of three components: sedimentary organic carbon (S), mantle (M), and limestone (L), we adopt the classical three-component mixing model of Sano and Marty (1995) to assess carbon provenance. Using the following equations, the relative contributions (expressed as fractions, f) from the three sources can be determined:

$$\left(^{13}C/^{12}C\right)_m = f_M\left(^{13}C/^{12}C\right)_M + f_L\left(^{13}C/^{12}C\right)_L + f_S\left(^{13}C/^{12}C\right)_S;$$
$$1/\left(^{12}C/^3He\right)_m = f_M/\left(^{12}C/^3He\right)_M + f_L/\left(^{12}C/^3He\right)_L + f_S/\left(^{12}C/^3He\right)_S;$$
$$f_M + f_L + f_S = 1$$

where subscripts m, M, L, and S refer to the measured sample, the mantle, the limestone, and the sedimentary organic carbon, respectively. Using $\delta^{13}C_{CO_2}$ values of $-6.5‰$, $0‰$, and $-30‰$ for M, L, and S and $^{12}C/^3He$ ratios of 1.5×10^9, 1×10^{13}, 1×10^{13} for M, L, and S, respectively, we estimate that no mantle-derived CO_2 is in gas samples from the Bacha Lake with the fraction of CO_2 originating from sedimentary organic carbon exceeding 50% (Figs. 5&6). Thus, we infer that more than half of the CO_2 is likely to derive from methane oxidation or organic matter degradation because these gas samples contain a small amount of CH_4. In contrast, gas samples from other sites all contain certain amounts of mantle-derived CO_2 ($\sim16–\sim65\%$) (Fig. 6), especially for the gas sample from the Tanggula Mountain Depot containing 100% mantle-derived CO_2, which is consistent with the inferences from $\delta^{13}C_{CO_2}$ values and $CO_2/^3He$ ratios. The geothermal gas in southern Tibet is also characterized by mantle-derived CO_2 (Yokoyama et al., 1999; Zhao et al., 2002). The mantle-derived CO_2 discharge in the target area may be associated with the occurrence of the Hoh Xil–Jinsha River suture and the Cenozoic volcanism in northern Tibet (Deng and Sun, 1999; Li et al., 2011; Turner et al., 1993). From Early Triassic to Late Jurassic, the Qiangtang Basin was filled by marine sediments dominated by marls and marly carbonate beds (Guo et al., 2008), and crustal thickening and large-scale magmatic intrusion resulting from intensive crustal shortening in the Tanggula–Tuotuo River area characterized by strong tectonic compression (Fu et al., 2010a; Li et al., 2011). Therefore, the decarbonation of carbonates resulting from magmatic activity is possibly the main contributor of limestone-derived CO_2 in gas samples.

5.3. Source of CH4

Methane produced in most sedimentary basins is generally classified as either being of microbial or thermogenic origin, i.e. related respectively to metabolic and biosynthetic activity of bacteria or thermal degradation of sedimentary organic matter (Schoell, 1988; Welhan, 1988; Whiticar, 1999). Abiotic methane, formed by chemical reactions that are not related to the existence of organic matter, is produced in much smaller amounts on a global scale. The occurrence of economically exploitable abiotic methane reservoirs has not been found apart from rare exceptions (Dai et al., 2005; Etiope and Lollar, 2013; Jin et al., 2009), which have been controversially discussed. $\delta^{13}C$ vs. δD plot has been proven to be an effective tool to unravel the sources of methane within certain limits (Schoell, 1980; Welhan, 1988; Whiticar, 1999), but we are not able to utilize this method, because no obtain δD values
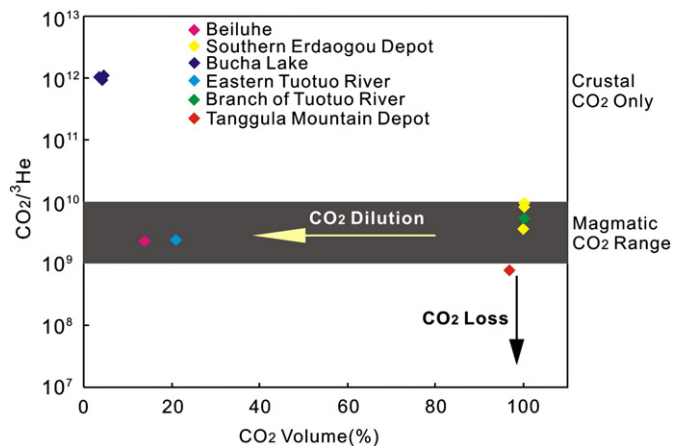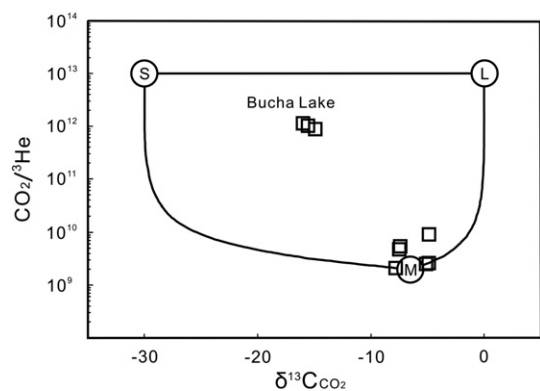

Fig. 4. Plot of $CO_2/^3He$ against CO_2 volume for all of the gas samples studied. The shade region highlights the range of $CO_2/^3He$ values of magmatic samples (Gilfillan et al., 2008). All error bars are smaller than plotted symbols.

Fig. 5. Plot of $CO_2/^3He$ versus $\delta^{13}C$ of CO_2 for gas samples. S, M, and L represent the sedimentary organic carbon, the mantle carbon, and the limestone. The end-member compositions for S, M, and L are $\delta^{13}C = -30$, -6.5, and $0‰$; and $CO_2/^3He = 1 \times 10^{13}$, 2×10^9, and 1×10^{13}, respectively (Sano and Marty, 1995). The data are explained by a 3-component mixing model between S–M–L. CO_2 from the Bucha Lake show a significant input of S and M end-members and CO_2 from the Beiluhe, the southern Erdaogou, the eastern Tuotuo River, and the branch of Tuotuo River mainly clusters close to the end-member M. All error bars are smaller than plotted symbols.
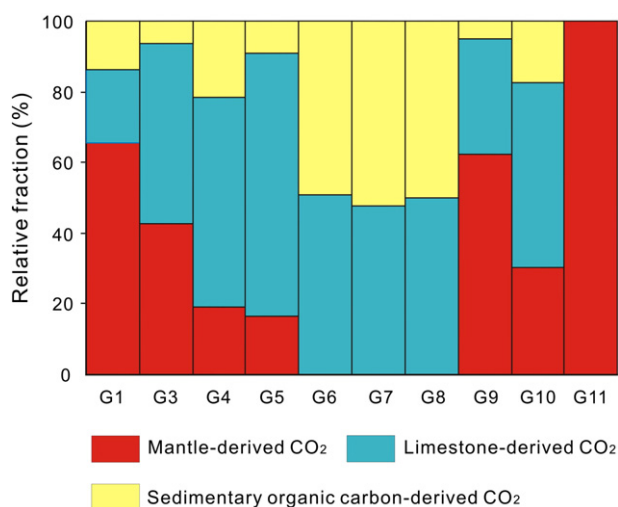
Fig. 6. Relative fraction of CO_2 calculated from S–M–L three-component mixing model.

from our samples are available. Meanwhile, overlapping ranges of $\delta^{13}C$ values from biotic and abiotic methane have been reported as pointed out by several studies (Horita and Berndt, 1999; McCollom and Seewald, 2006; McCollom et al., 2010; Taran et al., 2010) suggesting that abiotic CH_4 produced by gas–water–rock reactions can result in values as depleted as −57‰, which was previously assumed to be an indicator for biotic CH_4. The $\delta^{13}C$ values alone thus, do not enable a clear differentiation between biotic and abiotic methane sources. Hence, $CH_4/^3He$ ratios are adopted to further investigate fluid origins in the present study. Mantle-derived fluids typically have $CH_4/^3He$ values between 10^5 and 10^8, while $CH_4/^3He$ values of crust-derived fluid are much higher ranging from 10^8 to 10^{11} (Dai et al., 2005; Giggenbach et al., 1993). $CH_4/^3He$ values of gases from the Beiluhe (5.9×10^7), the eastern Tuotuo River (3.4×10^7), and the Tanggula Mountain Depot (1.2×10^7) indicate that CH_4 may be dominantly mantle-derived. In addition, there is a positive correlation between the $\delta^{13}C_1$ values and the abundance of mantle-derived He (Tables 1&2), possibly suggesting a mantle-derived CH_4 input. Although it has been traditionally assumed that abiotic CH_4 is mainly associated with mantle-derived or magmatic processes, new data show that relatively low-temperature synthesis related to gas–water–rock reactions is more common (Etiope and Lollar, 2013). Mantle-derived or magmatic CH_4 is abiotic, but not all abiotic CH_4 is mantle-derived. Thus, we can at least conclude that CH_4 from the Beiluhe, the eastern Tuotuo River, and the Tanggula Mountain Depot is abiotic. Notably, gas samples were collected from hot springs in the Tanggula Mountain Depot which is a major geothermal system of the Qiangtang Basin. The CH_4 thus, may be generated by abiotic reduction of the mantle-derived CO_2, comparable with the abiotic CH_4 discharging from the geothermal systems of the peri-Tyrrhenian area, Italy (Tassi et al., 2012). The CH_4 in gas samples collected from the Bucha Lake is referred to be crustal-derived with $CH_4/^3He$ values ranging from 5.9×10^9 to 1.65×10^{10}. Because mud bubbling was observed in some of the fluid releasing outlets and most of the CO_2 is inferred to stem from organic matter and contain no mantle information in the Bucha Lake, we postulate that the CH_4 is possibly also originated from organic matter and the biotic gas discharge might be linked to mud volcanism. It has been demonstrated that the seepage of biotic hydrocarbon is widespread in the hinterland of the Qiangtang Basin (Nan et al., 2008) while the CH_4 from our study area is mainly abiotic. The proximity to the Hoh Xil–Jinsha River suture and the possible influence by the Cenozoic volcanism may explain the difference of gas geochemistry between the oil seepage sites in the central Qiangtang Basin and our sampling sites which are primarily located along the eastern margin of the northern Qiangtang depression.

6. Conclusions

Although a myriad of lines of evidence have demonstrated that the Qiangtang Basin is the most favorable sedimentary basin for hydrocarbon and gas hydrate exploration and exploitation in the Qinghai–Tibet Plateau (Chen et al., 2005; Ding et al., 2013; Fu et al., 2010b, 2013; He et al., 2012), we did not see many surface hydrocarbon manifestations in the study area. Instead, CO_2 in gas samples from the Beiluhe, the southern Erdaogou Depot, the eastern Tuotuo River, the branch of Tuotuo River, and the Tanggula Mountain Depot at least partially originates from the mantle. In particular, all CO_2 from the Tanggula Mountain Depot seems to be derived from mantle sources, comparable with the geothermal gas discharge in southern Tibet. Meanwhile, the trace amount of abiotic CH_4 from Tanggula Mountain Depot is possibly produced by abiotic reduction of the mantle-derived CO_2. Only CO_2 and CH_4 from the Bucha Lake are inferred to be primarily biotic and are possibly linked to mud volcanism. The large-scale emission of mantle-derived CO_2 discovered in gas samples is likely to be associated with the occurrence of a regional deep-seated fault (Hoh Xil–Jinsha River suture) and the Cenozoic volcanism in northern Tibet. However, the limited discharge of mantle-derived He (2.15–5.66%) may be caused by the limited degree of openness at the bottom of fault zones and possibly reflects a geological setting of strong extrusion and crustal thickening.

References

Andrews, J.N., 1985. The isotopic composition of radiogenic helium and its use to study groundwater movement in confined aquifers. Chem. Geol. 49, 339–351.

Battani, A., Sarda, P., Prinzhofer, A., 2000. Basin scale natural gas source, migration and trapping traced by noble gases and major elements: the Pakistan Indus basin. Earth Planet. Sci. Lett. 181, 229–249.

Bräuer, K., Kämpf, H., Strauch, G., 2009. Earthquake swarms in non-volcanic regions: what fluids have to say. Geophys. Res. Lett. 36, L17309. http://dx.doi.org/10.1029/2009GL039615.

Cai, L., Zhonghua, H., Deming, Y., 1996. The problems of geological tectonics in the Qiangtang Area. World Geol. 15, 18–23.

Chen, D.F., Wang, M.C., Xia, B., 2005. Formation condition and distribution prediction of gas hydrate in Qinghai-Tibet Plateau permafrost. Chin. J. Geophys. 48, 179–187.

Craig, H., Lupton, J., Horibe, Y., 1978. A mantle helium component in circum-Pacific volcanic gases: Hakone, the Marianas, and Mt. Lassen, in terrestrial rare gases. In: Alexander, E.G., Ozima, M. (Eds.), Proceedings of the U.S.–Japan Seminar on Rare Gas Abundance and Isotopic Constraints on the Origin and Evolution of the Earth's Atmosphere. Center for Academic Publications Japan, Tokyo, pp. 3–16.

Crossey, L.J., Karlstrom, K.E., Springer, A.E., Newell, D., Hilton, D.R., Fischer, T., 2009. Degassing of mantle-derived CO_2 and He from springs in the southern Colorado Plateau region-neotectonic connections and implications for groundwater systems. Geol. Soc. Am. Bull. 121, 1034–1053.

Dai, J., Song, Y., Dai, C., Liao, Y., Chen, A., 1995. Conditions Governing the Formation of Abiogenic Gas and Gas Pools in Eastern China. Science Press, Beijing.

Dai, J.X., Yang, S.F., Chen, H.L., Shen, X.H., 2005. Geochemistry and occurrence of inorganic gas accumulations in Chinese sedimentary basins. Org. Geochem. 36, 1664–1688.

Deng, W., Sun, H., 1999. Relationship between Cenozoic volcanism in the Qinghai–Tibet Plateau and its uplifting (in Chinese with English abstract). Geol. Rev. 45, 952–958.

Ding, W., Wan, H., Zhang, Y., Han, G., 2013. Characteristics of the Middle Jurassic marine source rocks and prediction of favorable source rock kitchens in the Qiangtang Basin of Tibet. J. Asian Earth Sci. 66, 63–72.

Etiope, G., Klusman, R.W., 2002. Geologic emissions of methane to the atmosphere. Chemosphere 49, 777–789.

Etiope, G., Lollar, B.S., 2013. Abiotic methane on earth. Rev. Geophys. 51, 276–299.

Etiope, G., Feyzullayev, A., Baciu, C.L., 2009. Terrestrial methane seeps and mud volcanoes: a global perspective of gas origin. Mar. Pet. Geol. 26, 333–344.

Fu, X., Wang, J., Tan, F., Chen, M., Chen, W., 2010a. The Late Triassic rift-related volcanic rocks from eastern Qiangtang, northern Tibet (China): age and tectonic implications. Gondwana Res. 17, 135–144.

Fu, X., Wang, J., Zeng, Y., Tan, F., He, J., 2010b. Concentrations and modes of occurrence of platinum group elements in the Shengli River oil shale, northern Tibet, China. Fuel 89, 3623–3629.

Fu, X., Wang, J., Tan, F., Feng, X., Wang, D., He, J., 2013. Gas hydrate formation and accumulation potential in the Qiangtang Basin, northern Tibet, China. Energy Convers. Manag. 73, 186–194.

Giggenbach, W.F., Sano, Y., Wakita, H., 1993. Isotopic composition of helium, and CO2 and CH4 contents in gases produced along the New Zealand part of a convergent plate boundary. Geochim. Cosmochim. Acta 57, 3427–3455.

Gilfillan, S., Ballentine, C.J., Holland, G., Blagburn, D., Lollar, B.S., Stevens, S., Schoell, M., Cassidy, M., 2008. The noble gas geochemistry of natural CO2 gas reservoirs from the Colorado Plateau and Rocky Mountain provinces, USA. Geochim. Cosmochim. Acta 72, 1174–1198.

Graham, D.W., 2002. Noble gas isotope geochemistry of mid-ocean ridge and ocean island basalts: characterization of mantle source reservoirs. Rev. Mineral. Geochem. 47, 247–317.

Guo, Z., Li, Y., Nan, Z., Ye, H., 2008. Relationship between deformation structure and petroleum accumulation and preservation, Qiangtang Basin, Tibet. Pet. Explor. Dev. 35, 563–568.

He, J., Wang, J., Fu, X., Zheng, C., Chen, Y., 2012. Assessing the conditions favorable for the occurrence of gas hydrate in the Tuonamu area Qiangtang basin, Qinghai–Tibetan, China. Energy Convers. Manag. 53, 11–18.

Hoke, L., Lamb, S., Hilton, D.R., Poreda, R.J., 2000. Southern limit of mantle-derived geothermal helium emissions in Tibet: implications for lithospheric structure. Earth Planet. Sci. Lett. 180, 297–308.

Holland, G., Ballentine, C.J., 2006. Seawater subduction controls the heavy noble gas composition of the mantle. Nature 441, 186–191.

Horita, J., Berndt, M.E., 1999. Abiogenic methane formation and isotopic fractionation under hydrothermal conditions. Science 285, 1055–1057.

Hou, Z., Li, Z., 2004. Possible location for underthrusting front of the Indus Continent: constraints from helium isotope of the geothermal gas in southern Tibet and eastern Tibet (in Chinese with English abstract). Acta Geol. Sin. 4, 482–493.

Hu, D., Zhang, H., 1998. A preliminary study on the mud volcanic mechanism of Goujiumaiga Gully in Kekexili region, Qinghai–Xizang Plateau (in Chinese with English abstract). Arid Land Geogr. 21, 13–18.

Huang, J., 2001. Tectonic characteristics and evolution of the Qiangtang Basin. Reg. Geol. China 20, 178–186 (in Chinese with English abstract).

Jin, Z., Zhang, L., Wang, Y., Cui, Y., Milla, K., 2009. Using carbon, hydrogen and helium isotopes to unravel the origin of hydrocarbons in the Wujiaweizi area of the Songliao Basin, China. Episodes 32, 167–176.

Judd, A.G., Hovland, M., 2007. Seabed Fluid Flow: The Impact of Geology, Biology and the Marine Environment. Cambridge Univ Pr.

Kapp, P., Yin, A., Manning, C.E., Harrison, T.M., Taylor, M.H., Ding, L., 2003. Tectonic evolution of the early Mesozoic blueschist-bearing Qiangtang metamorphic belt, central Tibet. Tectonics 22, 1701–1725.

Li, Y., Wang, C., Ma, C., 2011. Balanced cross-section and crustal shortening analysis in the Tanggula–Tuotuohe Area, northern Tibet. J. Earth Sci. 22, 1–10.

Lollar, B.S., Ballentine, C.S., 2009. Insights into deep carbon derived from noble gases. Nat. Geosci. 2, 543–547.

Lu, Z., Wu, B., Rao, Z., Zhu, Y., Luo, X., Bai, R., 2007. Geological and geochemical anomalies of gas hydrate in permafrost zones along Qinghai–Tibet Railway, China (in Chinese with English abstract). Geol. Bull. China 26, 1029–1040.

Marty, B., Jambon, A., 1987. C/³He in volatile fluxes from the solid Earth: implications for carbon geodynamics. Earth Planet. Sci. Lett. 83, 16–26.

McCollom, T.M., Seewald, J.S., 2006. Carbon isotope composition of organic compounds produced by abiotic synthesis under hydrothermal conditions. Earth Planet. Sci. Lett. 243, 74–84.

McCollom, T.M., Lollar, B.S., Lacrampe-Couloume, G., Seewald, J.S., 2010. The influence of carbon source on abiotic organic synthesis and carbon isotope fractionation under hydrothermal conditions. Geochim. Cosmochim. Acta 74, 2717–2740.

Morrison, P., Pine, J., 1955. Radiogenic origin of the helium isotopes in rock. Ann. N. Y. Acad. Sci. 62, 71–92.

Nan, Z., Li, Y., Guo, Z., 2008. Hydrocarbon show and correlation between oil and source rock in the Qiangtang Basin (in Chinese with English abstract). Pet. Geol. Exp. 30, 503–507.

O'Nions, R., Oxburgh, E., 1988. Helium, volatile fluxes and the development of continental crust. Earth Planet. Sci. Lett. 90, 331–347.

Oxburgh, E., O'nions, R., Hill, R., 1986. Helium isotopes in sedimentary basins. Nature 324, 632–635.

Ozima, M., Podosek, F.A., 2002. Noble Gas Geochemistry. Cambridge University Press, London.

Porcelli, D., Ballentine, C.J., Wieler, R., 2002. An overview of noble gas — geochemistry and cosmochemistry. In: Porcelli, D., Ballentine, C.J., Wieler, R. (Eds.), Noble Gases in Geochemistry and Cosmochemistry, pp. 1–19.

Poreda, R., Craig, H., 1989. Helium isotope ratios in circum-Pacific volcanic arcs. Nature 338, 473–478.

Sano, Y., Marty, B., 1995. Origin of carbon in fumarolic gas from island arcs. Chem. Geol. 119, 265–274.

Schoell, M., 1980. The hydrogen and carbon isotopic composition of methane from natural gases of various origins. Geochim. Cosmochim. Acta 44, 649–661.

Schoell, M., 1988. Multiple origins of methane in the earth. Chem. Geol. 71, 1–10.

Shen, L., Yuan, D., Ding, T., Li, Y., Le, G., Lin, Y., 2007. Distribution inhomogeneity of helium isotope of CO2 degassification point and its geotectogenesis in southwest of China (in Chinese with English abstract). Acta Geol. Sin. 81, 475–487.

Sherwood Lollar, B., Ballentine, C., Onions, R., 1997. The fate of mantle-derived carbon in a continental sedimentary basin: integration of CHe relationships and stable isotope signatures. Geochim. Cosmochim. Acta 61, 2295–2307.

Song, Y., Xu, Y., 2005. Origin and identification of natural gases (in Chinese with English abstract). Pet. Explor. Dev. 32, 24–29.

Taran, Y., Kliger, G., Cienfuegos, E., Shuykin, A., 2010. Carbon and hydrogen isotopic compositions of products of open-system catalytic hydrogenation of CO2: implications for abiogenic hydrocarbons in earth's crust. Geochim. Cosmochim. Acta 74, 6112–6125.

Tassi, F., Fiebig, J., Vaselli, O., Nocentini, M., 2012. Origins of methane discharging from volcanic-hydrothermal, geothermal and cold emissions in Italy. Chem. Geol. 310, 36–48.

Turner, S., Hawkesworth, C., Liu, J.Q., Rogers, N., Kelley, S., Vancalsteren, P., 1993. Timing of Tibetan uplift constrained by analysis of volcanic rocks. Nature 364, 50–54.

Wang, C., Yi, H., 2001. Geologic Evolution and Hydrocarbon Prospect Evaluation of Qiangtang Basin (in Chinese). Geological Publishing House, Beijing.

Wang, J., Tan, F., Li, Y., Li, Y., Chen, M., Wang, C., Guo, Z., Wang, X., Du, B., Zhu, Z., 2004. The Potential of Oil and Gas Resources in Major Sedimentary Basins on the Qinghai–Xizang Plateau (in Chinese with English abstract). Geological Publishing House, Beijing.

Welhan, J.A., 1988. Origins of methane in hydrothermal systems. Chem. Geol. 71, 183–198.

Whiticar, M.J., 1999. Carbon and hydrogen isotope systematics of bacterial formation and oxidation of methane. Chem. Geol. 161, 291–314.

Wycherley, H., Fleet, A., Shaw, H., 1999. Some observations on the origins of large volumes of carbon dioxide accumulations in sedimentary basins. Mar. Pet. Geol. 16, 489–494.

Xia, G., 2009. The meter-scale sedimentary cycles and its forming mechanisms of middle Jurassic Xiali Formation in eastern Qiangtang Basin, Tibet (in Chinese with English abstract). Chengdu University of Technology, Chengdu.

Xie, C., Li, C., Li, L., Wu, Y., Hu, P., 2009. First discovery of mud volcanoes in central Qiangtang Basin, northern Tibet, China (in Chinese with English abstract). Geol. Bull. China 28, 1319–1324.

Xu, Y., Shen, P., Liu, W., Tao, M., 1996. Geochemistry of mantle-derived volatiles in natural gas from oil and gas provinces in eastern China — II Helium, argon, and hydrocarbons in mantle volatiles (in Chinese with English abstract). Sci. China Ser. D 26, 187–192.

Xu, Y., Liu, W., Shen, P., Tao, M., Zheng, J., 2003. An important branch of gas geochemistry–noble gas geochemistry (in Chinese with English abstract). Nat. Gas Geosci. 14, 157–166.

Xu, S., Nakai, S., Wakita, H., Wang, X.B., 2004. Carbon and noble gas isotopes in the Tengchong volcanic geothermal area, Yunnan, southwestern China. Acta Geol. Sin. Engl. Ed. 78, 1122–1135.

Xu, S., Zheng, G., Xu, Y., 2012. Helium, argon and carbon isotopic compositions of spring gases in the Hainan Island, China. Acta Geol. Sin. Engl. Ed. 86, 1515–1523.

Yang, T.F., 2008. Recent progress in the application of gas geochemistry: examples from Taiwan and the 9th International Gas Geochemistry Conference. Geofluids 8, 219–229.

Yang, T.F., 2013. Regional and tectonic application of gas/fluid geochemistry. J. Asian Earth Sci. 65, 1–2.

Yang, T.F., Lan, T.F., Lee, H.F., Fu, C.C., Chuang, P.C., Lo, C.H., Chen, C.H., Chen, C.T.A., Lee, C.S., 2005. Gas compositions and helium isotopic ratios of fluid samples around Kueishantao, NE offshore Taiwan and its tectonic implications. Geochem. J. 39, 469–480.

Yang, T.F., Marty, B., Hilton, D.R., Kurz, M.D., 2009. Geochemical applications of noble gases. Chem. Geol. 266, 1–3.

Yang, T.F., Hilton, D.R., Italiano, F., Heinicke, J., 2010. Applications of fluid and gas geochemistry for geohazards investigation. Appl. Geochem. 25, 503–504.

Ye, X., Tao, M., Yu, C., Zhang, M., 2007. Helium and neon isotopic compositions in the ophiolites from the Yarlung Zangbo River, Southwestern China: the information from deep mantle. Sci. China Ser. D Earth Sci. 50, 801–812.

Yokoyama, T., Nakai, S., Wakita, H., 1999. Helium and carbon isotopic compositions of hot spring gases in the Tibetan Plateau. J. Volcanol. Geotherm. Res. 88, 99–107.

Zhao, Z., Li, Y., Ye, H., 2001. Tectonic characteristics and basin evolution of Qinghai–Tibetan Plateau (in Chinese with English abstract). Science Publishing House, Beijing.

Zhao, P., Xie, E., Dor, J., Jin, J., Hu, X., Du, S., Yao, Z., 2002. Geochemical characteristics of geothermal gases and their geological implications in Tibet (in Chinese with English abstract). Acta Pet. Sin. 18, 539–550.

Zhao, W., Zhao, X., Shi, D., Liu, K., Jiang, W., Wu, Z., Xiong, J., Zheng, Y., 2004. Progress in the study of deep profiles of Tibet and the Himalayas (Indepth). Acta Geol. Sin. Engl. Ed. 78, 931–939.

Zhu, Y., Lu, Z., Xie, X., 2011. Potential distribution of gas hydrate in the Qinghai–Tibetan Plateau. Geol. Bull. China 30, 1918–1926.